

Analysis of Power Cycling Capability of IGBT Modules in a Conventional Matrix Converter

Lixiang Wei, Richard A Lukaszewski
 Rockwell Automation – Allen Bradley,
 6400 West Enterprise Drive,
 Mequon, WI, 53092, USA
lwei@ra.rockwell.com

Thomas A Lipo
 Department of Electrical and Computer Engineering
 University of Wisconsin-Madison
 1415 Engineering Drive, Madison,
 WI, 53706, USA

Abstract — this paper analyzes the power cycling capability of IGBT modules in a conventional matrix converter used as a motor drive. The analysis is made under various condition for this topology, including low speed operation capability, high speed thermal and power cycle capability and etc. It was found that the power cycling Mean Time to Failure (MTTF) of IGBT in a matrix converter is low when the input and output frequency is close to each other or when the output frequency of the converter is low. As a result, the chip size of the conventional matrix converter may be larger than the other candidates. In the end of the paper, some guidance of designing a matrix converter for long term reliabilities is also discussed.

Keywords – power cycle, thermal cycle, conventional matrix converter, Mean Time to Failure (MTTF)

I. INTRODUCTION

The conventional matrix converter has been introduced to the world for over twenty years [1]-[5]. The pros and cons of this converter has been studied thoroughly and compared with the most widely used rectifier-inverter system, such as voltage/current quality, control schemes, efficiencies, reliabilities and etc. Comparing to the rectifier-inverter system, it has the following advantages: adjustable input power factor, bi-directional power flow, high quality input/output waveforms, and the possibility of a compact design due to the lack of large energy storage component [1]. Figure.1 shows a conventional matrix converter topology with back to back IGBT connection for each switching cell.

One disadvantage of the matrix converter is that it has much more numbers of power switches than other topologies. Since power semiconductor is one of the most costly components in a converter, it is beneficial to investigate the long term reliability and the sizing of the semiconductors used in the matrix converter. The end of life period of complex multi-chip modules is often defined by the thermo-mechanical failure mechanisms [6][7][8]. Two of most important failure schemes have been carried out – power cycling and thermal cycling capability. The power cycling capability defines wear out mechanisms of the bond-wire on the silicon chip. It is closely related the temperature cycling of the silicon die during the working condition. The thermal cycling capability classifies the failure mechanism of the solder layer where the substrate of the module is soldered on the base-plate. It is determined by the temperature variation of the base plate during the overall working condition.

This paper investigates the power cycling capability of the IGBT being used in a matrix converter. Firstly, the losses calculation of the IGBT and diode under various conditions are studied. Then, a simplified electrical thermal cycle of a matrix converter is built up and the temperature cycles are studied under various condition. After that, the power cycle and thermal cycle capability of the IGBT under various operating condition are studied and compared. It is concluded that MTTF of the IGBT is low when the input and output frequency the matrix converter are close to each other or when the output frequency of the converter is low. As a consequence, a bigger IGBT module may have to be selected in order to guarantee an acceptable life expectation for a matrix converter.

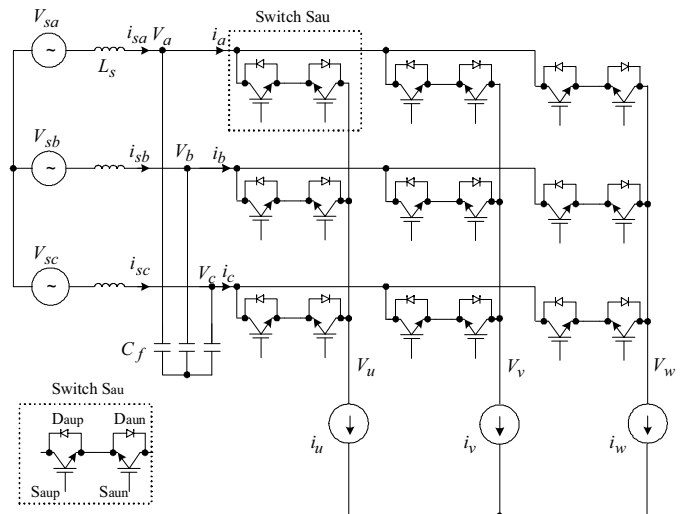


Figure 1. The conventional matrix converter topologies

II. CIRCUIT AND SYSTEM CONFIGURATION

In order to simplify the analysis, it is assumed that there is no input filter in the input of the matrix converter, thus, the following equations can be obtained from figure.1.

$$L_s = 0; C_f = 0; V_{sx} = V_x, i_{sx} = i_x \quad (1)$$

Where

L_s/C_f is the filter inductance/capacitance

x: input phase name, can be phase A, B or C

V_{sx}, i_{sx} : phase x source voltage and current

V_x, i_x : phase x converter side voltage and current

It is assumed that the input source voltage and output load are both balanced. The input voltage \bar{V}_s and output current \bar{i}_o are represented as:

$$\begin{aligned}\bar{V}_s &= \sqrt{\frac{2}{3}}(V_{sa} + \alpha \cdot V_{sb} + \alpha^2 \cdot V_{sc}) = V_m e^{j\omega_i t} \\ \bar{i}_o &= \sqrt{\frac{2}{3}}(i_u + \alpha \cdot i_v + \alpha^2 \cdot i_w) = i_{om} e^{j(\omega_o t + \phi_i)}\end{aligned}\quad (2)$$

where, $\alpha = e^{j2\pi/3}$, V_m and i_{om} are the per phase input voltage and output current amplitude respectively. ω_i and ω_o are the angular frequency of the input and output of the converter respectively. ϕ_i is the initial angle of the output current.

Another attractive character of the matrix converter is that a unity power factor can be achieved from the input side. Under this condition, the maximum voltage transfer ratio can be achieved. In this paper, it is assumed that the matrix converter is controlled under unity input power factor. Then, the following assumption can be made:

$$\begin{aligned}\bar{i}_s &= i_m e^{j\omega_i t} \quad \bar{i}_s = i_m e^{j\omega_i t} \\ \bar{V}_o &= V_{om} e^{j(\omega_o t + \phi_o)}\end{aligned}\quad (3)$$

where, ϕ_v is the angle of the converter output voltage.

III. POWER LOSSES CALCULATION OF IGBT/DIODES

A three phase matrix converter is studied to drive an induction motor. The information of the matrix converter is defined as:

Input line voltage: 480Vac line to line
Output frequency: 0Hz ~ 60Hz
Switching frequency: 4 kHz,
Output rated voltage: 415Vac line to line voltage
Rated current: 65Arms
IGBT module: FS100R12KE3

Due to the theory of the symmetry, only the IGBT/Diode losses of S_{aup} , S_{aun} , and D_{aup} , D_{aun} in switch S_{au} in figure.1 will be analyzed. The similar power losses curves can be derived for all other IGBTs and Diodes.

A. PWM control and duty ratio d_1 , d_2 calculation

Various PWM control method has been discussed for the matrix converter. In this paper, a similar PWM method as shown in reference [11] will be discussed.

The basic commutation method as discussed in [11] separates the matrix converter into six intervals according to input source voltage as shown Figure.2 (a). In each PWM cycle, two portions are separated as shown in Figure.2 (b). In this figure, Duty ratio d_1 and d_2 are calculated from the input voltage synchronization angle and can keep the input current waveform to be sinusoidal. The detailed calculation of d_1 and d_2 are listed in Table. I.

In each portion, the matrix converter can be simplified as a traditional inverter as described in Figure.2 (c). In this figure, V_{sx} and V_{sy} are the two of the three input phase voltages. The name of these two voltages in each portion and the corresponding commutation voltage are listed in Table. I.

In this table: $\theta_a, \theta_b, \theta_c$ are the commanded current angle of phase A, B and C respectively, where

$$\theta_a = \omega_i t; \theta_b = \omega_i t - \frac{2\pi}{3}; \theta_c = \omega_i t - \frac{4\pi}{3}\quad (4)$$

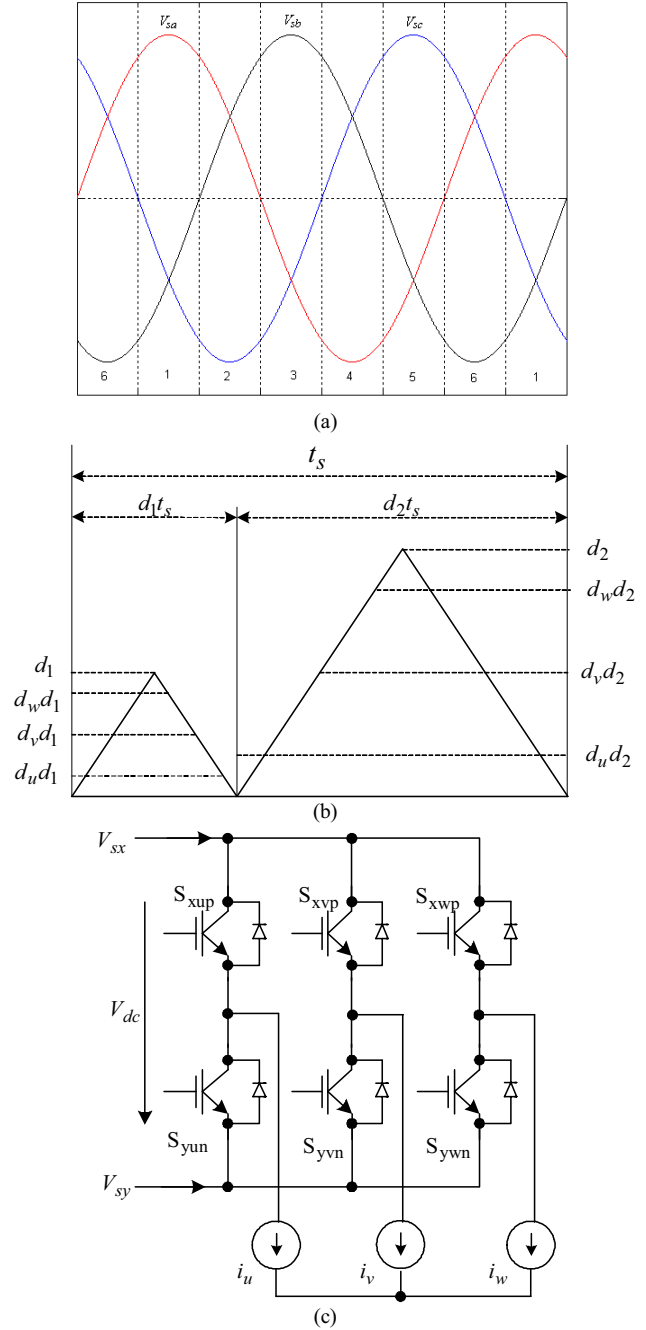


Figure 2. Six intervals for switching sequence and two portions in each PWM cycle. (a) six intervals based on input voltage, (b) two portions and its duty cycles in each switching cycle, (c) equivalent circuit of the matrix under each portion (x, y are two of the three input voltage terminals as listed in table. I)

TABLE I. DUTY RATIO CALCULATION AND COMMUTATION VOLTAGES IN EACH PORTION

interval	Portion 1				Portion 2			
	d_1	V_{sx}	V_{sy}	V_{dc}	d_2	V_{sx}	V_{sy}	V_{dc}
1	$-\frac{\cos\theta_b}{\cos\theta_a}$	V_{sa}	V_{sb}	V_{sab}	$-\frac{\cos\theta_c}{\cos\theta_a}$	V_{sa}	V_{sc}	V_{sac}
2	$-\frac{\cos\theta_b}{\cos\theta_c}$	V_{sb}	V_{sc}	V_{sbc}	$-\frac{\cos\theta_a}{\cos\theta_c}$	V_{sa}	V_{sc}	V_{sac}
3	$-\frac{\cos\theta_c}{\cos\theta_b}$	V_{sb}	V_{sc}	V_{sbc}	$-\frac{\cos\theta_a}{\cos\theta_b}$	V_{sb}	V_{sa}	V_{sba}
4	$-\frac{\cos\theta_c}{\cos\theta_a}$	V_{sc}	V_{sa}	V_{sca}	$-\frac{\cos\theta_b}{\cos\theta_a}$	V_{sb}	V_{sa}	V_{sba}
5	$-\frac{\cos\theta_a}{\cos\theta_c}$	V_{sc}	V_{sa}	V_{sca}	$-\frac{\cos\theta_b}{\cos\theta_c}$	V_{sc}	V_{sb}	V_{sbc}
6	$-\frac{\cos\theta_a}{\cos\theta_b}$	V_{sa}	V_{sb}	V_{sab}	$-\frac{\cos\theta_c}{\cos\theta_b}$	V_{sc}	V_{sb}	V_{sbc}

B. Duty ratio d_u , d_v and d_w calculation

Duty ratios d_u , d_v and d_w are directly derived from the output voltage command vector. In this paper, a third order harmonics is added to the duty ratios to increase the voltage transfer ratio. The following duty ratio value can be defined:

$$\begin{aligned}
 d_u &= \frac{1}{2} + \frac{k}{2} \left[\cos(\omega_o t + \varphi_v) - \frac{1}{4} \cos(3\omega_o t + 3\varphi_v) \right] \\
 d_v &= \frac{1}{2} + \frac{k}{2} \left[\cos(\omega_o t + \varphi_v - \frac{2\pi}{3}) - \frac{1}{4} \cos(3\omega_o t + 3\varphi_v) \right] \\
 d_w &= \frac{1}{2} + \frac{k}{2} \left[\cos(\omega_o t + \varphi_v + \frac{2\pi}{3}) - \frac{1}{4} \cos(3\omega_o t + 3\varphi_v) \right]
 \end{aligned} \tag{5}$$

where, k is the voltage modulation index level of the converter and it is proportional to the ratio between output voltage and input voltage

C. Duty ratio and conduction losses calculation of S_{au}

Combining Table I and Eq.4, the duty ratio of S_{aup} can be calculated as

$$d_{au} = \begin{cases} d_u & -\frac{\pi}{6} \leq \theta_a < \frac{\pi}{6} \\ d_2 d_u & \frac{\pi}{6} \leq \theta_a < \frac{5\pi}{6} \\ d_u & \frac{5\pi}{6} \leq \theta_a < \frac{7\pi}{6} \\ d_1 d_u & \frac{7\pi}{6} \leq \theta_a < \frac{11\pi}{6} \end{cases} \tag{6}$$

According to Figure.1, the IGBT S_{aup} and D_{aun} conducts only when phase U current is positive and when switch S_{au}

turns on. On the other hand, S_{aun} and D_{aup} conduct only when phase U current is negative and when switch S_{au} is turned on.

The conduction losses of S_{aup} and D_{aup} can be calculated by

$$\begin{aligned}
 P_c(S_{aup}) &= \begin{cases} d_{au}(V_t + R_t i_u) i_u & i_u > 0 \\ 0 & i_u \leq 0 \end{cases} \\
 P_c(D_{aup}) &= \begin{cases} 0 & i_u > 0 \\ d_{au}(V_t + R_t i_u) i_u & i_u \leq 0 \end{cases}
 \end{aligned} \tag{7}$$

where, $P_c(S_{aup})$ and $P_c(D_{aup})$ are the conduction losses of S_{aup} and D_{aup} respectively; V_t and R_t are the threshold voltage and slope resistance of IGBT S_{aup} ; V_d and R_d are the threshold voltage and slope resistance of Diode D_{aup} .

Figure.3 (a) and(b) illustrates the average conduction losses of S_{aup} and D_{aup} under motoring and regenerating condition.

D. Switching losses of S_{aup} and D_{aup}

In each portion, the matrix converter can be simplified as a three phase DC/AC inverter by keeping only six switches switching in each portion. Then, the switching losses can be generated for switching S_{aup} and D_{aup} when either V_{sx} or V_{sy} in Figure.2 (b) is represented by phase A. When input phase A appears to be V_{sx} as shown in Figure.2 (b) and phase U current is positive. The switching losses will be generated on S_{aup} . In contrary, when phase U current is negative, the switching losses will be generated on D_{aup} .

Combining Table I, the switching losses of S_{aup} can be calculated as

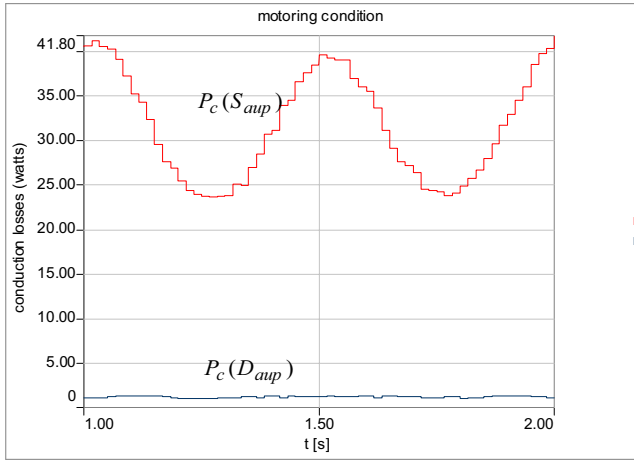
$$\begin{aligned}
 P_s(S_{aup}) &= \begin{cases} k_s V_{sab} i_u & \frac{9\pi}{6} \leq \theta_a < \frac{11\pi}{6} \text{ and } i_u > 0 \\ k_s (V_{sab} + V_{sac}) i_u & -\frac{\pi}{6} \leq \theta_a < \frac{\pi}{6} \text{ and } i_u > 0 \\ k_s V_{sac} i_u & \frac{\pi}{6} \leq \theta_a < \frac{3\pi}{6} \text{ and } i_u > 0 \\ 0 & \text{other cases} \end{cases} \\
 k_s &= \frac{E_{on} + E_{off}}{V_n I_n}
 \end{aligned} \tag{8}$$

where, k_s is a switching losses constant for the IGBT. E_{on} and E_{off} are the turn on and off losses respectively. V_n and I_n are the nominal voltage and current for the IGBT module.

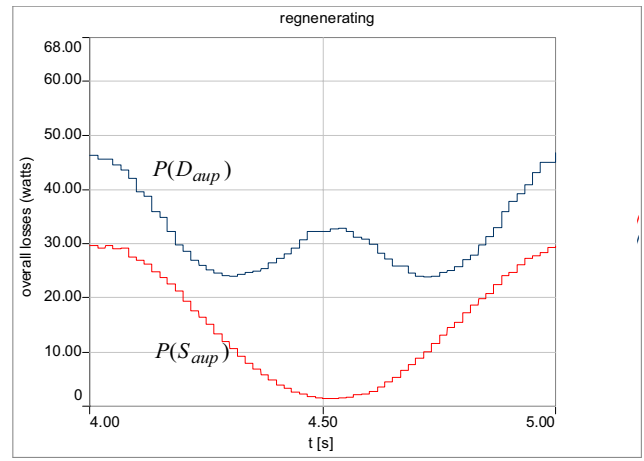
Similarly, the switching losses of D_{aup} can be calculated as

$$\begin{aligned}
 P_s(D_{aup}) &= \begin{cases} k_d V_{sab} |i_u| & \frac{9\pi}{6} \leq \theta_a < \frac{11\pi}{6} \text{ and } i_u < 0 \\ k_d (V_{sab} + V_{sac}) |i_u| & -\frac{\pi}{6} \leq \theta_a < \frac{\pi}{6} \text{ and } i_u < 0 \\ k_d \cdot V_{sac} |i_u| & \frac{\pi}{6} \leq \theta_a < \frac{3\pi}{6} \text{ and } i_u < 0 \\ 0 & \text{other cases} \end{cases} \\
 k_d &= E_{rec} / V_n I_n
 \end{aligned} \tag{9}$$

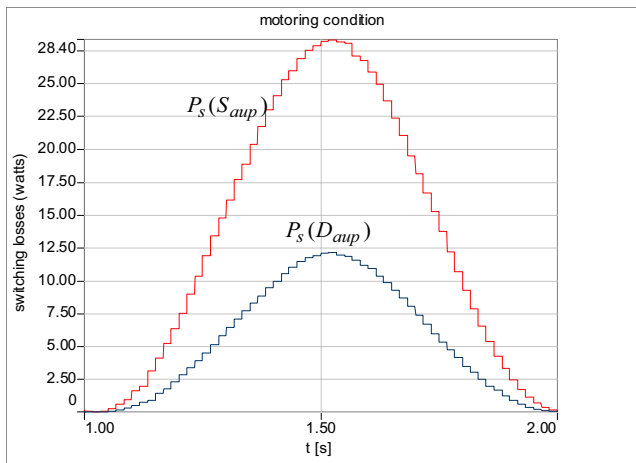
where, k_d is the switching losses constant for the diode. E_{rec} is the reverse recovery losses of the diode from the datasheet.



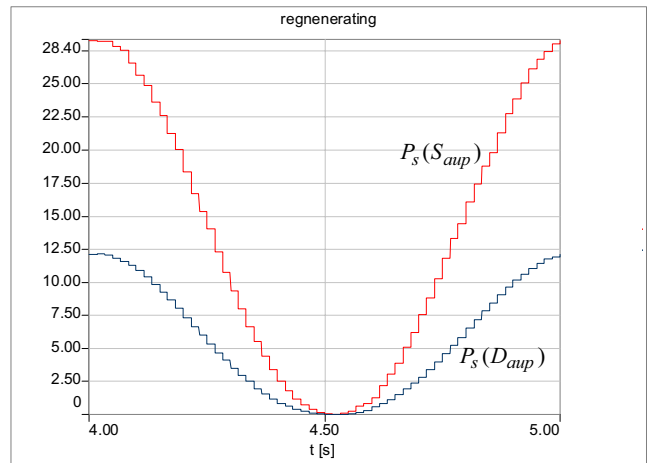
(a)



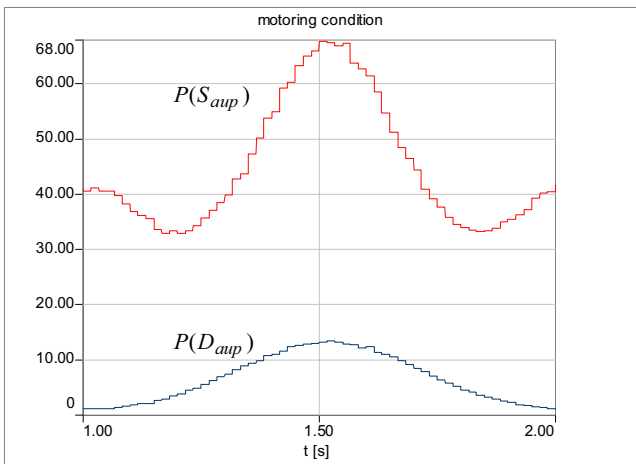
(b)



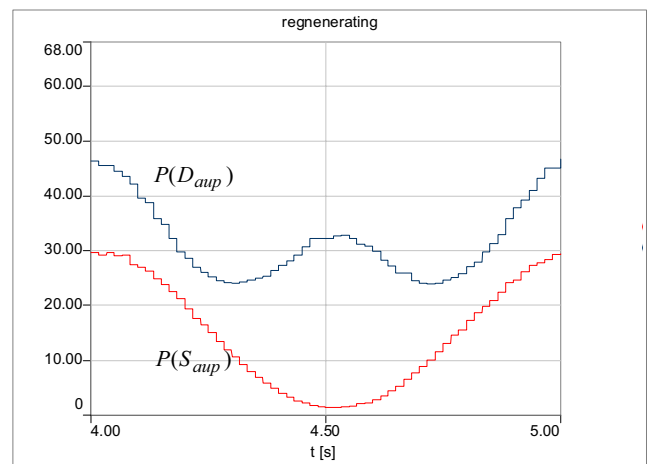
(c)



(d)



(e)



(f)

Figure 3. losses of S_{aup} and D_{aup} in every input cycle (input frequency: 60Hz, Output current/frequency: 65Arms/59Hz, $k = 1.732$, unity input/output power factor)
 (a): conduction losses at motoring condition, (b) conduction losses at regenerating condition, (c): switching losses at motoring condition, (d) switching losses at regenerating condition, (e): overall losses at motoring condition, (f) overall losses at regenerating condition.

E. Overall power losses of the S_{aup} and D_{aup}

Combining equation (7) ~ (9), the overall losses of S_{aup} and D_{aup} can be calculated as

$$P(S_{aup}) = P_c(S_{aup}) + P_s(S_{aup})$$

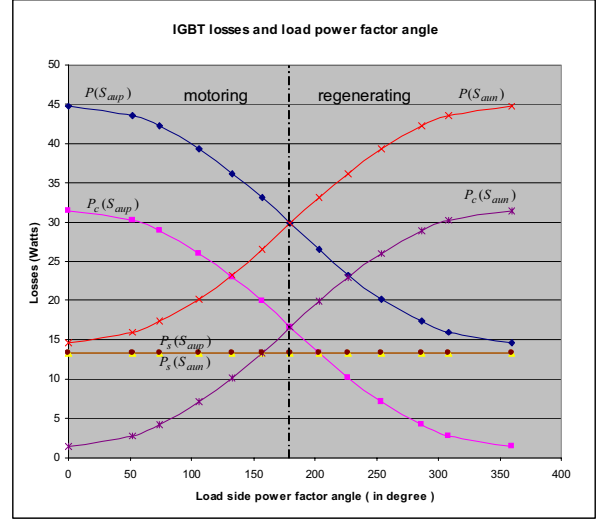
$$P(D_{aup}) = P_c(D_{aup}) + P_s(D_{aup}) \quad (10)$$

Figure.3 illustrates the average conduction, switching and overall losses of S_{aup} and D_{aup} under motoring and regenerating condition. In this figure, the losses are averaged in every input voltage source cycle (1/60Hz). The output load operates at 59Hz and rated current (65Arms).

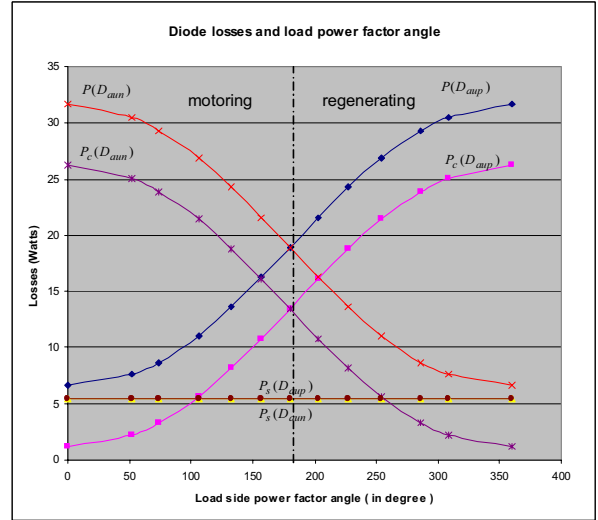
Figure.4 further demonstrates the average power losses of the S_{aup} , S_{aun} , D_{aup} and D_{aun} at various output power factor conditions. In this figure, all losses are averaged in every slip frequency between the input voltage source and output load frequency ($1/(f_i - f_o)$).

The following conclusion can be made from Figure.3 and 4.

- According to Figure.3 (a) and (b), the conduction losses of both switches in the matrix converter are modulated by a low frequency component. The frequency is approximately two times of the input and output slip frequency $2*(f_i - f_o)$.
- Figure.3 (c) and (d) demonstrates the switching losses of S_{aup} and D_{aup} at motoring and regenerating conditions. According to these two figures, the switching losses of the both switches are modulated by a low frequency component ($f_i - f_o$).
- From Figure.3 (c) and (d), the magnitude of the switching losses for both switches are similar to each other; however, a phase shift of the conduction losses and the switching losses can be seen between the motoring and regenerating condition of the converter.
- According to Figure.3 (e) and (f) and equation (10), it can be concluded that there are two low frequency components in the overall losses for both switches.
- According to Figure.3 (e) and (f), the overall losses of S_{aup} are much higher at motoring condition than that in the regenerating condition. In comparison, the overall losses of D_{aup} are much lower at motoring condition.
- Figure.4 demonstrates that the conduction losses of D_{aup} and S_{aun} are much lower at motoring condition and losses during the regenerating condition.
- If the characters of the load are defined, it is possible to size the S_{aup} , S_{aun} , D_{aup} , and D_{aun} appropriately to achieve the best price and performance ratio. For example, if a motoring load is designed, then the size of S_{aup} and D_{aun} can be much bigger than that of S_{aun} and D_{aup} .
- However, it is not possible to eliminate the number of switches as the dual bridge matrix converter shown in reference [13]. Under that case, as few as 9 switches are needed.



(a)



(b)

Figure 4. Average IGBT and Diode Losses as a function of load side power factor angle, (a): losses of IGBT S_{aup} and S_{aun} , (b) losses of Diode D_{aup} and D_{aun} ,

IV. THERMAL MODELLING OF THE MATRIX CONVERTER SYSTEM

A. Thermal Modelling of the Diode and IGBT chips

The thermal modeling of the Diode and IGBT chips in one heat-sink has been discussed by many articles. Figure.5 shows a simplified thermal system for the matrix converter systems. In this figure, Z_{jc} and Z_{jcd} are the thermal impedance between the junction and case layer of the IGBT and diode chip respectively. Z_{ch} and Z_{chd} are the thermal impedance between the case layer and the heat sink. The similar thermal impedance value as shown in [12] are applied. R_h and C_h are the thermal resistance and capacitance of the heat-sink.

The thermal resistance and time constants of the diode and IGBT chips are listed in Table. II. The thermal resistance and

time constants of the heat-sink are selected as $R_h = 0.06 \text{ k/w}$ and a time constants of $\tau_h = R_h C_h = 120 \text{ s}$

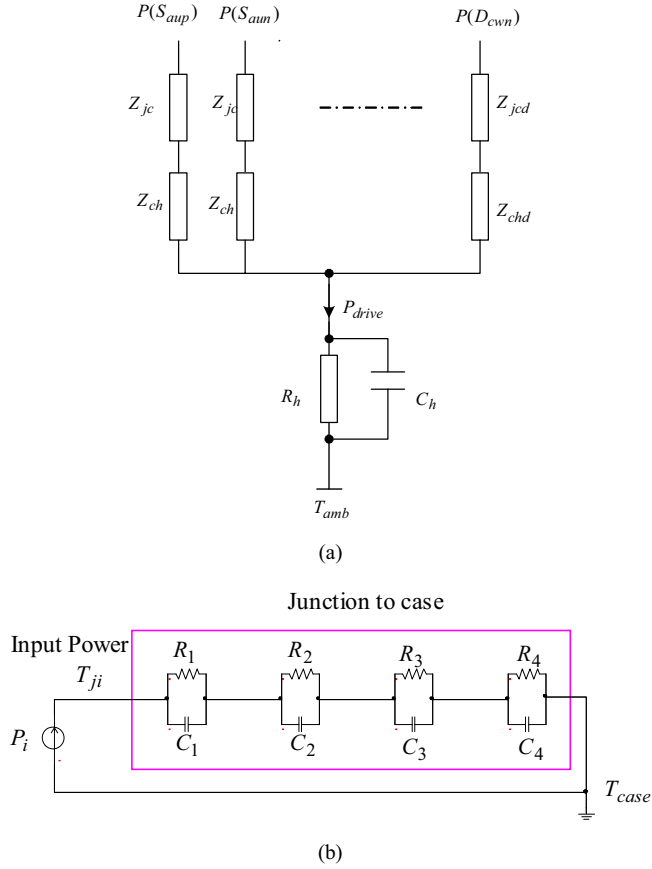


Figure 5. Simplified thermal system of the maxtrix converter system. (a) overall thermal network model, (b) thermal impedance between the junction and case layer of one chip.

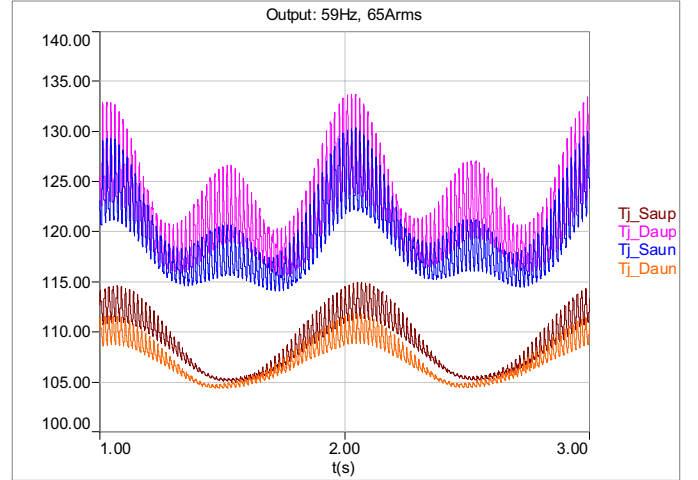
TABLE II. THERMAL IMPEDANCE OF THE TESTED IGBT/DIODE

Segments	1	2	3	4	Zch
Ri: (K/W)	0.00493	0.01501	0.13088	0.10919	0.13
τ_i : (s)	1.187e-5	0.002364	0.02601	0.06499	0.7
Rd: (K/W)	0.00908	0.02726	0.24202	0.20164	0.15
τ_d : (s)	1.187e-5	0.002364	0.02601	0.06499	0.7

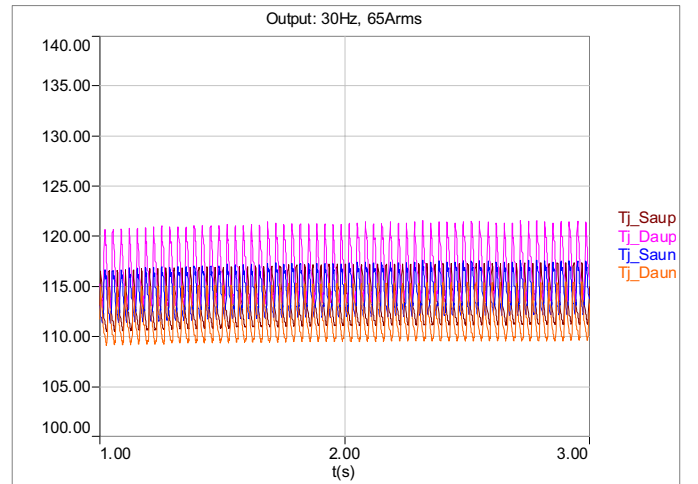
B. Junction temperature of IGBT and Diode under various input/ouput frequencies

With all above analysis, the junction temperatures of the IGBT and Diode chips in switch S_{au} under different output frequency are plotted.

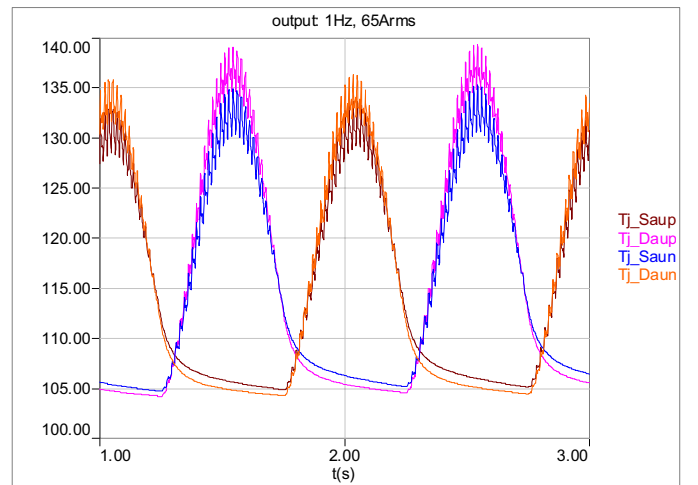
From Figure.6 (a), the input and output frequency of the converter has only 1Hz difference. A big temperature variation with a low frequency on each IGBT and Diode chips was shown when the input and output frequency of the converter is close to each other. Similarly, from Figure.6 (c), a low frequency variation can also be seen when the converter operates under low output frequency.



(a)



(b)



(c)

Figure 6. Junction temperature profile of the matrix converter under various output frequency. (input frequency: 60Hz, switching frequency: 4kHz) (a): output frequency: 59Hz, (b): output frequency 30Hz, (c) output frequency: 1Hz

V. POWER CYCLING MTTF CALCULATIONS

A. Failure Mode of the IGBT/Diode Chips and MTTF estimation of the module

Studies have shown that power cycling of the IGBT caused by the low cycle fatigue is one of the dominant failure mechanisms higher power IGBT multi-chip modules [6][7][8][9][10]. The driving force of the mechanism is the mismatch in the thermal expansion coefficients of aluminum and silicon. During operation, the junction temperature of each chip may increase or decrease quickly for more than 60°C. This produces a differential elongation of the bond-wire in respect to the substrate, and it results into a plastic flow of the wire material. Especially at the periphery of the bonding interface where the shear stress reaches its maximum strength.

A typical model of predicting the number to failure of the IGBT based power cycling capability has been studied in reference [9] as

$$N_f(T_m, \Delta T_j) = A \cdot \Delta T_j^\alpha \cdot \exp\left(\frac{Q}{R \cdot T_m}\right) \quad (11)$$

where, A, α , Q, R are all constant and is decided by way the module is built up, ΔT_j is the variation of the junction temperature, T_m is the mean junction temperature in one power cycle.

Based on the reliability data from the supplier, the following extracted values are used in this paper.

$$A = 654.8$$

$$\alpha = -7.801$$

$$Q/R = 1.378 \times 10^4 \text{ } ^\circ\text{C} \quad (12)$$

To predict the MTTF of the module under power cycling capability, one widely used method is called linear accumulation of the thermal cycle fatigue damage models as shown in reference [8]. Under this assumption, the mean time to failure (MTTF) of the bond-wires for a silicon chip can be estimated as:

$$MTTF = \frac{T}{\int_0^T \frac{N(T_m(t), \Delta T_j(t))}{N_f(T_m(t), \Delta T_j(t))} dt} \quad (13)$$

where T is the unit cycle time period of the load to be studied, $N(T_m(t), \Delta T_j(t))$ is the number of power cycles of the silicon die with an average junction of $T_m(t)$ and temperature variation of $\Delta T_j(t)$ in each period T. $N_f(T_m(t), \Delta T_j(t))$ is the number of cycles to failure of the chip under the same temperature condition.

Detailed description of how equation (13) is derived is beyond the scope of this paper and will not be discussed.

Due to the limitation of the laboratory setup, the MTTF study of matrix converter is not shown; however, the effectiveness of this approach has been verified successfully in a separate paper [14] to predict the lifetime of IGBT in a DC/AC inverter system by the same author.

B. Power Cycling MTTF Estimation of the Module under full load conditions

Based on the analysis above, the MTTF estimation of the IGBT module under full load is studied by combining equation (11) and (13). During the study, it is assumed that the converter operates at rate current 65Arms with a fixed load power factor (0.9). The output frequency of the converter is adjusted from 0.25Hz to 57.75Hz. The average temperature T_m and temperature variation ΔT_j of each frequency is simulated under Simplorer program and calculated in excel spread sheet.

Figure.7 further shows the MTTF estimation of S_{aup} and D_{aun} under the studied condition. From this figure, it can be found that the matrix converter has a much shorter life when the output frequency is close to input frequency or when the output frequency is low.

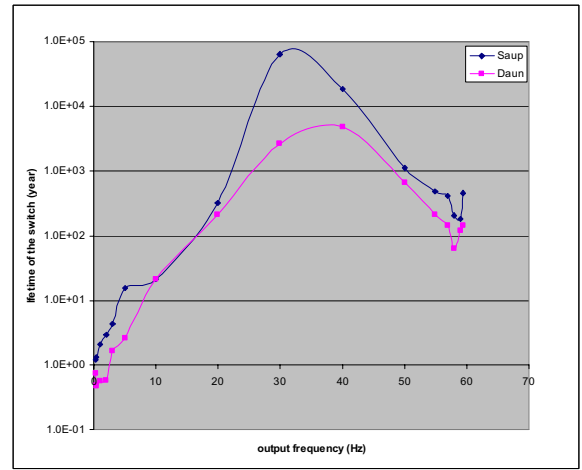


Figure 7. MTTF of S_{aup} and D_{aun} when the converter operates under rated output current and various output frequencies

C. Power Cycling MTTF Estimation of the Module under Repeated Overload Operating Conditions

The similar studies are made for the converter at repeated overload mode. Under this condition, the converter operates 50% overload (output current: 97.5Arms) for every 3 seconds and rated load (output current: 65Arms) for 57 seconds repeatedly as shown in Figure.8 (a).

Figure.8 (b) shows the MTTF estimation of S_{aup} and D_{aun} under the studied condition. From this figure, it can also be found that the matrix converter has a much shorter life when the output frequency is close to input frequency or when the output frequency is low.

From Figure.8 (b), the MTTF of the IGBT and Diode are very limited under overloaded condition. For example, when the output frequency is less than 10Hz, the life of the S_{aup} and D_{aun} is much less than 1 year. As a result, both IGBT and diode chips may have to be oversized in order to achieve an acceptable life.

D. Discussion

Based on above analysis, the following conclusions can be obtained.

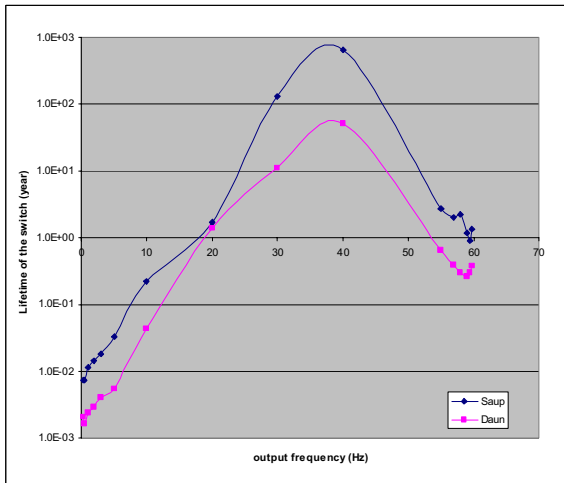
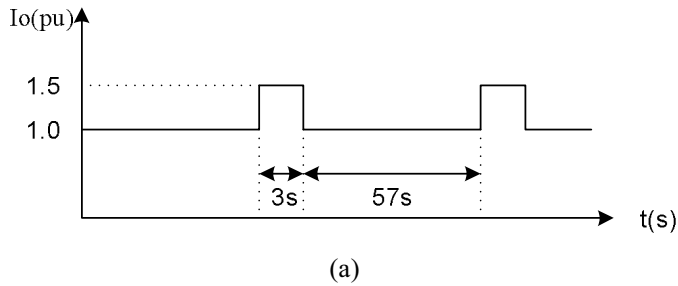


Figure 8. MTTF of S_{aup} and D_{aun} when the converter operates under rated output current and various output frequencies (input frequency: 60Hz, switching frequency: 4kHz) (a) output current curve, (b) MTTF of the switching

- The MTTF time of the matrix converter are low when the output frequency is low and when the input and output frequency are close to each other;
- The characteristics of the MTTF for both IGBT and Diode adds some disadvantages of sizing the silicon for matrix converter for fan, pump load which shows higher torque only when the output is high. More expensive silicon may have to be selected in order to guarantee an acceptable life for this converter.
- To optimize the silicon sizes in the matrix converter, a close studies has to be made on the load for power cycling capabilities. For examples, if converter works under regenerating mode for majority of the time, the sizes of S_{xyn} / D_{xyp} : $x = (a, b, \text{ or } c)$, $y = (u, v, \text{ or } w)$ can be largely smaller than that of S_{xyp} / D_{xyn} .
- The other way to improve the long term reliability of the matrix converter is to find a different PWM commutation method which will allow much less switching losses in the IGBT/Diodes chips at these two severe conditions.

VI. CONCLUSION

This paper calculates the losses and MTTF of the IGBT and Diode chips under matrix converters. The following conclusions can be made

- A higher temperature variation on the silicon chips can be seen when the output of the converter is low or when the input and output frequency are close to each other.
- The MTTF of the silicon chips are reduced under above two conditions. Thus, sizing of the silicon has to be properly made to avoid earlier failure of the converter
- This power cycling characteristic of matrix converter may further increase the silicon sizes and result in a higher silicon cost than other topologies.
- To optimize the silicon size of the matrix converter, the characters of the load has to be closely studied.
- When the converter output frequency is high and approaching the input frequency, The MTTF might be able to be improved by selecting a proper commutation scheme for the matrix converters. This is beyond the scope of this paper and will not be discussed.

VII. REFERENCES

- [1] M. Venturini, "A new sine wave out, conversion technique eliminates reactive component", in proc. PowerCon 7, 1980, pp E3-1-E3-15
- [2] Jang Hyoun Youm, and Bong Hwan Kwon, "Switching technique for current controller AC-to-AC converters," IEEE trans. On industrial Electronics, vol 46, No.2, 1999, pp.309-318
- [3] Mahlei J, Igney J, Braun M, Simon Olaf, "Robust matrix converter commutation without explicit sign measurement", EPE Graz 2001 CD ROM Paper 19.
- [4] Patrick W Wheeler, Jon C Clare, Lee Empringham and etc, "gate drive level intelligence and current sensing for matrix converter current commutation", IEEE Trans. On industrial electronics, vol.49, No.2, 2002, pp.382-389.
- [5] Vlatko Vlatkovic, and Dusan Borjevic, "Digital signal processor based control of three phase vector modulated converters", IEEE Trans. On Industrial Electronics, vol.41, No.3, 1994, pp.326-332
- [6] Mauro Ciappa, Flavio Carbognani, Wolfgang Fichner, "Lifetime prediction and design of reliability tests for high power devices in automotive applications, IEEE Trans. on Device and Materials Reliability, Vol.3, No.4, Dec, 2003, pp.191-196
- [7] Abhijit Dasgupta, "Failure mechanism models for cyclic fatigue", IEEE Transactions on Reliability, Vol.42, No.4, 1993, Dec. 2007.
- [8] Mauro Ciappa, and Wolfgang Fichtner, "lifetime prediction of IGBT modules for traction applications", In proc of IEEE 38th annual international reliability physics symposium, San Jose, California, 2000.
- [9] M. Held, P. Jacod, P.Scacco, and M. Poech, "Fast power cycling test for IGBT modules in traction application ", in proc IEEE APEC 1997, Georgia, USA.
- [10] A.T Bryant, PA Mawby, and etc, "Exploration of power devices reliability using compact device models and fast electro-thermal simulation", in proceedings of IEEE IAS 2006 conference CD, Tampa, Florida USA.
- [11] Lixiang Wei and Thomas A Lipo, "Robust voltage commutation of the conventional matrix converter", in proc. IEEE PESC'2003, Vol.2, June 15-19, pp.717-722.
- [12] Lixiang Wei, Russ J Kerkman, and etc, "Junction temperature prediction of a multi-chip IGBT module under DC condition ", in proc. IEEE IAS'2006, Oct. 2007, Florida, USA.
- [13] Lixiang Wei, Thomas A Lipo, "Matrix converter topologies with reduced number of switches", in proc. IEEE PESC'2002, June, 2002, Austria.
- [14] Lixiang Wei, Russ J Kerkman, Richard A Lukaszewski, "Evaluation of Power Semiconductor Power Cycling Capabilities for Adjustable Speed Drive", in proc. IEEE IAS 2008 conference CD, Edmonton, Canada, 2008.